Interaction of Cellulose, Hemicellulose, and Lignin During Co-Pyrolysis and their Effects on Pyrolysis Products

Kun Wang,[a] Xinhua Song,[a,*] Hongxiao Yu,[a,*] Tongxu Cui,[a] Jian Liu ,[b,c] Zelin He,[b] Mengying Chen,[a] and Binbin Yao [a]

* Corresponding author: xhs1111@sina.com; yhx168@sohu.com

DOI: 10.15376/biores.21.2.4207-4234

GRAPHICAL ABSTRACT

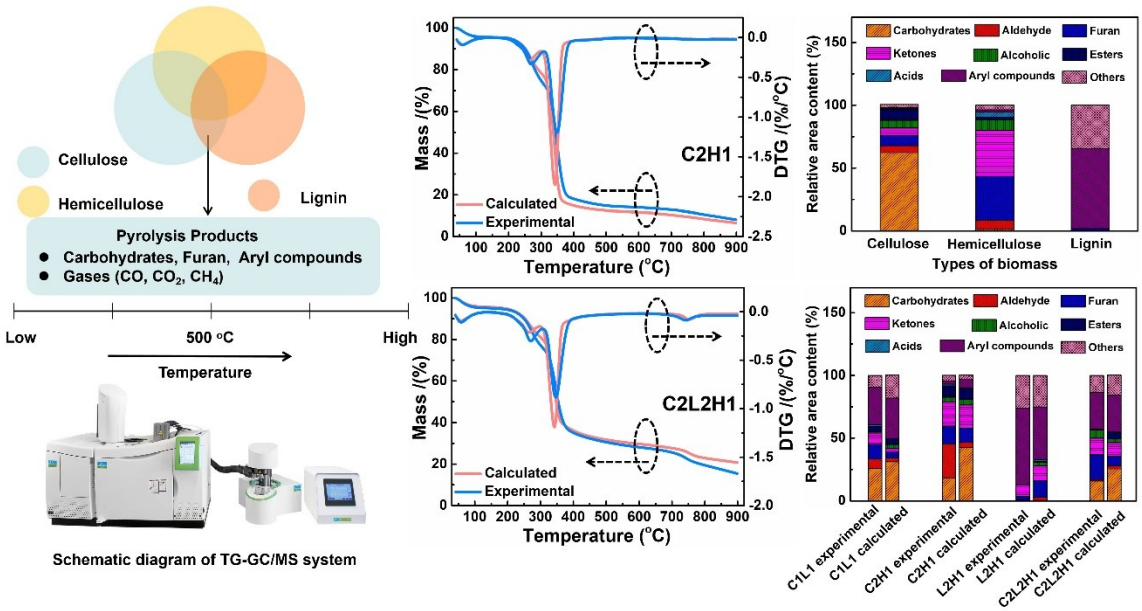

Interaction of Cellulose, Hemicellulose, and Lignin During Co-Pyrolysis and their Effects on Pyrolysis Products

Kun Wang,[a] Xinhua Song,[a,*] Hongxiao Yu,[a,*] Tongxu Cui,[a] Jian Liu ,[b,c] Zelin He,[b] Mengying Chen,[a] and Binbin Yao [a]

Biomass plays a vital role in alleviating the energy crisis and environmental pressure through its efficient conversion and utilization. Pyrolysis technology has become one of the core pathways for biomass resource utilization. However, the complex interactions among the three core components of biomass (cellulose, hemicellulose, and lignin) during the pyrolysis process complicate the in-depth analysis of biomass pyrolysis mechanisms and the optimization of pyrolysis processes. In this study, TG-GC/MS tandem technology was employed to systematically investigate the individual and co-pyrolysis characteristics of cellulose, hemicellulose, and lignin. The interactions between components were quantitatively analyzed by comparing experimental values with calculated superimposed values, and the distribution pattern of pyrolysis products was clarified through qualitative detection via GC/MS. The key findings were as follows: (1) due to the inherent characteristics of their chemical structures, the three components exhibit obvious differences in pyrolysis properties and characteristic products; (2) specific interactions exist between components during the co-pyrolysis process. By revealing the co-pyrolysis interactions between components and the product regulation mechanism, this research not only deepens the understanding of the intrinsic nature of biomass pyrolysis but also provides key data support and theoretical references for the high-value application of biomass pyrolysis technology.

DOI: 10.15376/biores.21.2.4207-4234

Keywords: Cellulose-hemicellulose-lignin; Co-pyrolysis; Interaction effect; Pyrolysis products

Contact information: a: China Tobacco Shandong Industrial Company Limited, Jinan 250104, China;
b: Institute of Tobacco Research, Chinese Academy of Agricultural Sciences, Qingdao 266101, China;
c: China Beijing Life Science Academy, Beijing 102209, China;
** Corresponding author: xhs1111@sina.com; yhx168@sohu.com*

INTRODUCTION

As one of the critical energy sources sustaining human survival, biomass accounts for approximately 14% of the world's total primary energy utilization and consumption. (Abbasi and Abbasi 2010). Therefore, the rational development and effective utilization of biomass energy are of great significance. The main methods of biomass resource utilization include combustion, gasification, and pyrolysis. Among them, the pyrolysis process has been widely used because it matches the characteristics of the biomass with respect to their high content of volatile components, low fixed carbon, and low cost (Rosillo-Calle 2016). Cellulose, hemicellulose, and lignin are the main components in biomass, which has the advantages of wide distribution, low cost, and renewability. They are complex polymer

compounds intertwined to form a highly integrated polymeric system (Wang *et al*. 2011; Stefanidis *et al*. 2014).

Biomass pyrolysis technology generally refers to the process in which the three major components are heated simultaneously at a high temperature under anaerobic or anoxic conditions. In such a process, their polymer structures are depolymerized to produce pyrolysis carbon, pyrolysis oil, and other pyrolysis by-products (Zhang *et al*. 2007). Based on different heating rates, pyrolysis processes can be divided into slow, medium, and high heating rates (Zhang *et al*. 2007). The three main chemical components differ in relative contents in different biomasses. In addition, biomass also contains small amounts of inorganics (ash) and organic extracts (McKendry 2002). Notably, during the practical resource utilization of biomass, these three components are almost always pyrolyzed as a naturally intertwined mixture rather than in isolation (Liu *et al*. 2020; Liu *et al*. 2024). This co-pyrolysis scenario involves not only the independent depolymerization of each component but also critical gas-phase interactions. Such interactions are essential for understanding why co-pyrolysis yields differ from the summed results of separate pyrolysis. Specifically, when cellulose, hemicellulose, and lignin undergo thermal decomposition simultaneously, their respective depolymerization processes release a range of monomeric/oligomeric organic compounds (*e.g.*, anhydrosugars from cellulose, furans from hemicellulose, and phenols from lignin) and free radicals (*e.g*., hydroxyl radicals, alkyl radicals) into the gas phase. These gaseous species can participate in a series of reactions (Wu *et al*. 2023). For example, anhydrosugars derived from cellulose may undergo cross-polymerization with furan-based compounds from hemicellulose, forming more complex oligomeric intermediates that ultimately affect the yield of pyrolytic oil components. Alternatively, free radicals generated from the cleavage of lignin's alkaryl ether bonds may act as catalysts or initiators, accelerating the decomposition of small-molecule oxygenates (*e.g*., hydroxyacetaldehyde) released by cellulose and thereby altering the distribution of gaseous products (Ye *et al*. 2017). Additionally, competitive reactions may occur between different gaseous species-for instance, hydroxyl radicals from cellulose decomposition might compete with phenoxy radicals from lignin for reaction sites, inhibiting the formation of certain phenolic monomers while promoting the generation of light alkanes. These gas-phase interactions directly modify the reaction pathways of individual components. Lignin and cellulose undergo pyrolysis to form oligomers, and hydrogen bond networks exist between these oligomers (Wu *et al*. 2014). Light fractions (such as free radicals) produced by cellulose pyrolysis undergo cross-polymerization reactions with heavy fractions generated from lignin pyrolysis, converting gaseous precursors into condensable liquids (*i.e*., bio-oil) (Li *et al*. 2021). Owing to the complexity of such individual pyrolysis behaviors and the aforementioned gas-phase interactions during co-pyrolysis, directly investigating the pyrolysis mechanism of real biomass (using raw biomass as the feedstock) remains challenging. Overlapping reactions cause interference, obscuring the contribution of each component to the final products. Therefore, it is necessary to first study the separate pyrolysis of the three major components to establish a baseline for their intrinsic thermal behaviors, before exploring their co-pyrolysis interactions. This sequential research approach is crucial for gaining a deeper understanding of the overall biomass pyrolysis mechanism and for optimizing pyrolysis conditions to enhance product quality and yield.

Cellulose is an abundant component in biomass (Marchessault and Sundararajan 1983). The structure of cellulose is relatively simple: the long-chain polymer of cellulose is formed by the β-D glucosyl group through 1,4 glycosidic bonds, which belong to the

homogeneous glycan group. The molecular formula of cellulose is $(C_6H_{10}O_5)_n$, where n is the degree of polymerization (Etale *et al*. 2023). The pyrolysis products of cellulose include dehydrated sugars and their derivatives, furans, small molecules of chain-like oxygenates, coke, and non-condensable gases (Brunner and Roberts 1980; Lédé *et al*. 2002; Lu *et al*. 2011). The relative contents of these products vary with the pyrolysis temperature, heating rate, and pyrolysis time. For example, Lu *et al*. (2011) analyzed a rapid pyrolysis process of cellulose, using Py-GC/MS to investigate the effects of the pyrolysis temperature and time on the pyrolysis products. In this rapid pyrolysis process, cellulose began to decompose at a set pyrolysis temperature of 400 °C to form organic volatile products. The pyrolysis products included various dehydrated sugars and their derivatives, furan compounds, light linear carbonyl compounds, and other compounds. The latter mainly consisted of anhydrosugars (dominated by the levoglucosan (LG)) and their derivatives (mainly the levoglucosenone (LGO), 1,4:3,6-dianhydro-D-glucopyranose (DGP), 1,5-anhydro-4-deoxy-d-glycero-hex- 1-en-3-ulose (APP) and 1-hydroxy-3,6-dioxabicyclo[3.2.1]octan-2one (LAC)), furan compounds (typically the 5-hydroxymethyl-furfural (HMF), furfural (FF) and furan (F)), as well as light linear carbonyls (mainly the hydroxyacetaldehyde (HAA) and 1-hydroxy-2- propanone (HA), *etc*.

Hemicellulose is a general term for a class of amorphous complex glycans, which are mainly composed of six basic sugar units, namely xylose, mannose, glucose, glucuronic acid, galactose, and arabinose (Lavarack *et al*. 2002). Due to the large differences in hemicellulose extracted from different biomasses and the difficulty of extraction, most studies on hemicellulose have been carried out using hemicellulose-modulated xylan (Guo *et al*. 2007). Hosoya *et al*. (2007b) carried out pyrolysis experiments on glucomannan and xylan under high temperature conditions. They studied the main pyrolysis products in tar. Their pyrolysis products of hemicellulose were mainly furans, while the yield of hydroxyl compounds of C_2 and C_3 was low. Shen *et al*. (2010) studied the pyrolysis path of xylan by detecting the pyrolysed gas and liquid products, *via* TG-FTIR and Py-GC-FTIR analyses.

Lignin is the most stable component of the three major components of biomass and has the largest span of pyrolysis intervals. It is an amorphous biomolecule with a very complex chemical structure and biopolymorphisms (Parthasarathi *et al*. 2011). The basic structural unit of lignin is phenylpropane, which consists of three basic structures: p-coumaryl, coniferyl, and sinapyl alcohols. The corresponding precursors are p-hydroxyphenyl (H), guaiacyl (G), and syringyl (S), respectively (Argyropoulos *et al*. 2002). Phenolic monomers, the main products of lignin pyrolysis, can be obtained by cleavage of aryl and alkyl ether bonds, and these main products will undergo secondary reactions at high temperatures. Furthermore, some of the products will form small molecule oxygenated compounds such as acetic acid, methanol, light alkanes, and aromatic polymers, *etc*. (Kuroda *et al*. 1990; Gooty *et al*. 2014; Kim *et al.* 2014).

To understand the pyrolysis characteristics of biomass, researchers have conducted a lot of studies on single component biomasses of cellulose, hemicellulose, and lignin. After the pyrolysis behavior of the three main components has been clarified, the pyrolysis behavior of a biomass can be predicted through the superposition of products according to its content of each component. However, a large deviation has been observed between the real product distribution and the theoretical result obtained by superposition (Hosoya *et al*. 2007a). Interactions of biomass components in the course of pyrolysis, therefore, are important and demand dedicated investigations. However, such investigations have been very limited and often yield inconsistent conclusions (Hosoya *et al*. 2007a; Dorez *et al.* 2014). The current work investigated the single and co-pyrolysis characteristics of

cellulose, hemicellulose, and lignin, and probe into the underlying mechanisms *via* a TGA-GC/MS coupled method, which is capable of both qualitative and quantitative analysis.

EXPERIMENTAL

Instruments and Reagents

The TG (TGA 8000, PerkinElmer, USA)-GC/MS (Clarus 690/Clarus SQ 8T, PE, USA) tandem instrument from PerkinElmer was used. Among the single-component materials used in this experiment, cellulose (CAS number: 9004-34-6, purchased from Sigma-Aldrich, USA) and lignin (CAS number: 8061-51-6, purchased from TCI, Japan) were commercial powdered samples. Hemicellulose was a laboratory-extracted sample from tobacco, and it was also preprocessed into a powder after extraction. Cellulose was derived from biomass, followed by chemical modifications, purification, and mechanical pulverization for preparation. Lignin was first prepared from biomass *via* sodium sulfite treatment, followed by chemical modifications such as partial desulfonation, oxidation, hydrolysis, and demethylation. The preparation method of hemicellulose was as follows: first, ethanol was used to remove pigments and organic impurities from tobacco leaves. Subsequently, an alkaline hydrolysis reaction was carried out using an aqueous sodium hydroxide solution. The filtrate was neutralized to pH 7 with hydrochloric acid, after which absolute ethanol was added to the feed solution for alcohol precipitation. The obtained intermediate was bleached with hydrogen peroxide, followed by a second alcohol precipitation process using absolute ethanol, and finally, filtration was performed to obtain the target hemicellulose. Meanwhile, their average particle sizes were measured using a laser particle size analyzer (Mastersizer 3000; Inaba and Matsumoto 1999), which were 64.7 μm, 51.7 μm, 70.3 μm, respectively. Prior to the initiation of the experiment, the moisture contents of cellulose, lignin, and hemicellulose were determined *via* the oven method (Bowden 1984), yielding values of 5.00%, 4.44%, and 4.76%, respectively. These reagents were not treated before the experimental work.

To prepare the mixed samples, the single-component cellulose, lignin, and hemicellulose were weighed separately first. Subsequently, these components were mixed and stirred thoroughly to ensure the homogeneity of the mixed samples. After confirming uniform mixing, the samples were placed into ceramic crucibles for the subsequent TGA-GC/MS experiments. The mass ratios of the mixed samples (cellulose-lignin, cellulose-hemicellulose, lignin-hemicellulose, and cellulose-lignin-hemicellulose) were determined with reference to the typical content ratios of the three components in flue-cured tobacco and other common biomass feedstocks (Saura-Calixto *et al*. 1983; Weng *et al*. 2024). Specifically, the mass ratios were set as follows: cellulose: lignin =1:1 (denoted as C1L1), cellulose: hemicellulose =2:1 (denoted as C2H1), lignin: hemicellulose =2:1 (denoted as L2H1), and cellulose: lignin: hemicellulose =2:2:1 (denoted as C2L2H1). All experiments in this research were repeated three times (n=3).

Thermogravimetric (TG) Method

First, 10 mg of cellulose, hemicellulose, lignin, and mixed powder samples of cellulose-lignin, cellulose-hemicellulose, lignin-hemicellulose, and cellulose-lignin-hemicellulose were weighed and put into alumina crucibles. These samples were heated from 40 to 900 °C at a heating rate of 10 °C/min, and then naturally cooled down to room temperature after pyrolysis. The pyrolysis atmosphere was nitrogen with a flow rate of 40

mL/min. During the TG heating process, the pyrolysis products were blown into a gas chromatography-mass spectrometry (GC-MS) for analysis using a 70 mL/min nitrogen atmosphere.

GC-MS Method

By analyzing the TG data, volatile products of the samples at the temperature with the maximum weight loss rate were collected for GC/MS analysis. The GC conditions were set as follows: An Elite-5MS capillary column (30 m× 0.25 mm ID×0.25 μm df) was used as chromatographic column. The inlet temperature was 250 °C. The carrier gas was He (purity of 99.999%) with flow rate at 1 mL/min, and the split ratio was 10:1. The heating curve was set as follows: firstly the temperature was kept at 50 °C for 5 min; then the temperature was raised to 150 °C at 3 °C/min and held for 1 min. Then the temperature was raised further to 250 °C at 10 °C/min and was held at 250 °C for 8 min. The MS conditions, on the other hand, included a 230 °C set temperature for the electron impact ion source (EI, 70 eV), a full scan mode with a scan range of 45 to 450 m/z, and a solvent delay time of 1 min. To prevent condensation of volatile products when they were blown into GC-MS, the temperatures of the transmission line and inlet were set to 270 °C.

Prediction of Co-pyrolysis Process and Product Distribution

Equation 1 was used to determine the distribution of the products during a co-pyrolysis process, based on the superimposition rule and the mixed ratios of cellulose, lignin, and hemicellulose. The interaction between cellulose, lignin, and hemicellulose during the co-pyrolysis was analyzed by comparing the experimental and calculated values of $Y_{calc,\,i}$ (Wang *et al.* 2008; Stefanidis *et al.* 2014), which is the theoretical value of the thermal weight loss rate of the sample, or the theoretical value of the relative area content of pyrolysis product i. $Y_{calc,\,i}$ was determined as follows,

$$Y_{calc,\,i} = Y_{cellulose,\,i} \times X_{cellulose} + Y_{lignin,\,i} \times X_{lignin} + Y_{hemicellulose,\,i} \times X_{hemicellulose} \quad (1)$$

where $Y_{cellulose,\,i}$ $Y_{lignin,\,i}$ and $Y_{hemicellulose,\,i}$ refer to the real thermal weight loss values of the pyrolysis of single-component cellulose, lignin and hemicellulose, respectively, or the experimental value of cellulose/lignin/hemicellulose pyrolysis product i. $X_{cellulose}$, X_{lignin}, and $X_{hemicellulose}$ are the mass proportions of cellulose, lignin and hemicellulose in the mixed sample, respectively.

RESULTS AND DISCUSSION

Single Pyrolysis Characteristics of Cellulose, Lignin, and Hemicellulose

Figure 1 shows the TG and DTG profiles of single cellulose, lignin, and hemicellulose at a heating rate of 10 ℃/min in an N_2 atmosphere, while Table 1 summarizes the key characteristic parameters of their individual pyrolysis processes. There were distinctive differences in the pyrolysis behavior of the three macromolecules. As observed in Fig. 1 and Table 1, hemicellulose exhibited typical pyrolysis characteristics: its initial pyrolysis temperature was 74 °C, with major weight loss initiating at approximately 200 °C and corresponding to a temperature for the maximum weight loss rate (T_{max}) of 266 °C, which was the lowest among the three components. This confirms that hemicellulose is the most easily decomposable constituent. In contrast, cellulose initiated pyrolysis at 304 °C. With increasing temperature, its mass decreased rapidly,

reaching the maximum weight loss rate at 341 °C. Pyrolysis was nearly complete at 437 °C, leaving a final solid residue of only 3.23%, which is consistent with the data reported in the literature (Shafizadeh and Fu 1973; Zhang *et al*. 2021). Lignin, however, displayed pyrolysis behavior over a wide temperature range, with weight loss primarily occurring between 76 and 778 °C. This process encompasses free water removal, rapid pyrolysis (generating small-molecule and macromolecular condensable gases), and deep pyrolysis carbonization (Liu *et al*. 2008). The maximum weight loss rate of lignin at 344 °C was 0.21%/°C, much lower than that of cellulose (2.85%/°C), and its final solid residue accounted for 42.47% (with a total weight loss of 57.53%), in agreement with the findings by Jin *et al* (2016).

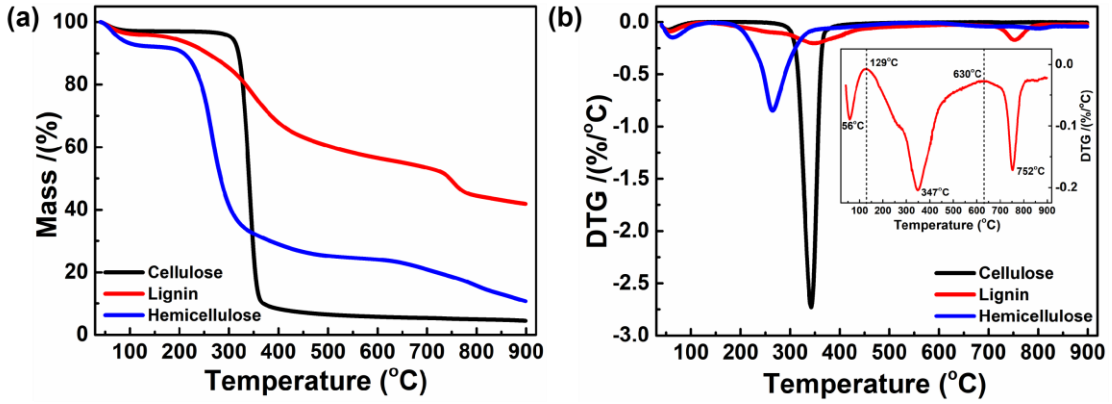

Fig. 1. Pyrolysis curves of cellulose, lignin, and hemicellulose. (a) TG curves, (b) DTG curves

Table 1. Parameters of Pyrolysis of Cellulose, Lignin, and Hemicellulose

Sample	T_{in} (°C)	T_{end} (°C)	T_{max} (°C)	DTG_{max} (%/°C)	Residue (%)
Cellulose	304±1a	437±88a	341±2b	-2.85±0.18a	3.23±1.88a
Lignin	76±2b	778±12b	344±3b	-0.21±0.01b	42.47±0.53b
Hemicellulose	74±7b	800±29b	266±3a	-0.89±0.07c	10.98±5.13c

T_{in}, the starting temperature of pyrolysis, defined as the temperature point when the total mass loss has reached 5%.
T_{end}, the end temperature of pyrolysis, defined as the temperature point when the total mass loss has reached 95%.
T_{max}, the temperature yielding the maximum weight loss rate.
Residue refers to the residual mass of the sample when the temperature has reached 900 °C.
Values in the same row with different columns indicate significant difference ($P<0.05$) according to Duncan's tests.

Thus, the order of pyrolysis reactivity is determined as hemicellulose > cellulose > lignin (in terms of pyrolysis difficulty: lignin > cellulose > hemicellulose), which is primarily attributed to their structural differences. Hemicellulose possesses a random amorphous structure with low molecular chain strength, making it susceptible to hydrolysis by dilute acids or alkalis and resulting in the highest reactivity. Cellulose is a crystalline, unbranched long-chain polymer composed of glucose units; its rigid structure and hydrolysis resistance lead to a higher initial pyrolysis temperature and concentrated pyrolysis process. Lignin, consisting of three types of highly cross-linked phenylpropane units, exhibits ultra-high thermal stability and the lowest reactivity (Yang *et al*. 2006).

Notably, in terms of structural and chemical property differences, the residue content of cellulose should be higher than that of hemicellulose. However, this is inconsistent with the TG results presented in Fig. 1 and Table 1, which may be attributed to the variations in reactions or mechanisms involved in the pyrolysis process of different components (Dai *et al*. 2023; Yang *et al*. 2007). This phenomenon has been confirmed by Ball *et al*. (2004) through differential scanning calorimeter (DSC) tests. Specifically, the relatively high solid residue contents derived from the pyrolysis of hemicellulose are mainly associated with the exothermic peaks observed during pyrolysis, which are linked to carbonization reactions. In contrast, an endothermic peak is detected during cellulose pyrolysis; thus, its extremely low solid residue content is a consequence of rapid devolatilization reactions. Additionally, lignin and hemicellulose show a weak weight loss peak between 700 and 800 °C, no such peak is observed for cellulose.

Co-pyrolysis Characteristics of Cellulose, Lignin, and Hemicellulose Mixtures

Co-pyrolysis of cellulose and lignin

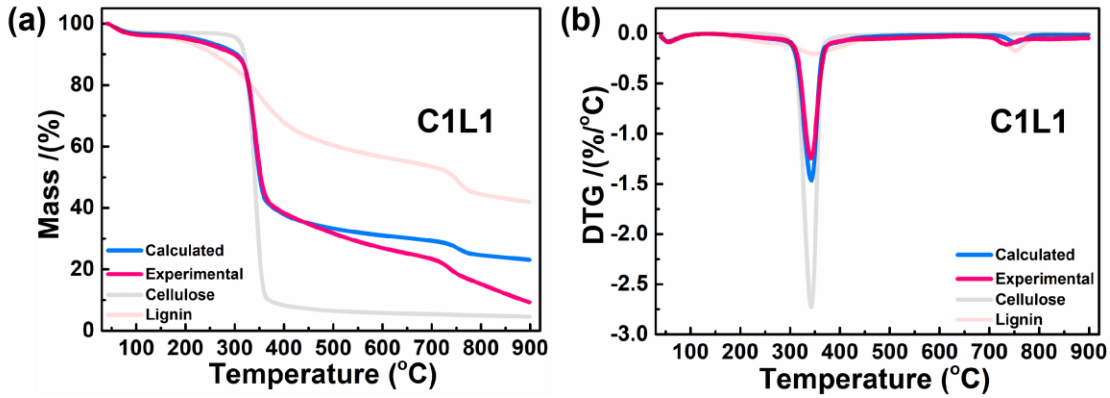

Fig. 2. Pyrolysis curves of cellulose, lignin and C1L1. (a) TG, (b) DTG

The interactions between cellulose, lignin, and hemicellulose vary depending on their relative content (Wu *et al*. 2023). Table 2 summarizes the parameters for the co-pyrolysis of mixtures of cellulose, lignin, and hemicellulose. Experimental and calculated thermal weight loss curves (TG and DTG curves) for the mixture of cellulose and lignin (C1L1) are shown in Fig. 2. The weight loss peak of co-pyrolysis of cellulose and lignin was in the same temperature range as that of cellulose, indicating that cellulose played a major role in the co-pyrolysis of cellulose and lignin. The weight loss rate of the mixture decreased significantly when compared with that of the single-component cellulose. Although the measured and calculated temperature yielding the maximum weight loss rate overlapped with each other, the experimental and calculated co-pyrolysis curves did show some discrepancies (Wu *et al*. 2014). For example, the calculated maximum weight loss rate (1.59%/°C) and residual weight (22.76%) were higher than those of the experimental results (1.22%/°C and 15.74%). Wu *et al*. (2016a, b) observed a similar phenomenon. It was confirmed that the co-pyrolysis of cellulose and lignin could increase the yield of small molecule products. This is because the interaction between cellulose and lignin helped produce a large number of gaseous products in the high temperature end, and the presence of cellulose inhibited the carbonization of these gaseous products, thereby reducing the production of solid residue (Hosoya *et al*. 2007a; Rosillo-Calle 2016). The interaction

between cellulose and lignin inhibited the decomposition of cellulose because the maximum weight loss rate of the cellulose-lignin mixture shifted from cellulose (2.85%/°C) to lignin (0.21%/°C), and the experimental maximum weight loss rate (1.22%/°C) was lower than the calculated value (1.59%/°C). These results indicated that the interaction between cellulose and lignin cannot be ignored in their co-pyrolysis process.

Co-pyrolysis of cellulose and hemicellulose

Experimental and calculated TG and DTG co-pyrolysis curves for the mixture of cellulose and hemicellulose (C2H1) are shown in Fig. 3a and 3b, respectively. Compared with the single component pyrolysis process, the co-pyrolysis of the C2H1 mixture started at 109 °C, and the TG curve became flat above 410 °C. At 720 °C, the co-pyrolysis process ended. There were two weight loss peaks in the DTG curve of the C2H1 mixture, and they intersected at 310 °C. The weight loss peak before 310 °C could be attributed to hemicellulose, while the weight loss peak after 310 °C was from cellulose. These observations indicate that hemicellulose and cellulose played a dominant role in the co-pyrolysis process before and after 310 °C, respectively. The calculated and experimental TG and DTG curves overlapped with each other before 310 °C, indicating that the effect of cellulose on the pyrolysis process of hemicellulose was weak. When the temperature was higher than 310 °C, the experimental DTG curve was significantly lower than the calculated one, which was consistent with the results of Liu *et al.* (2011). The experimental temperature of T_{end} (720 °C) was higher than the calculated T_{end} (669 °C). Furthermore, the residues of the two curves were not significantly different. Lastly, the calculated maximum weight loss rate (1.94%/°C) was higher than the experimental result (1.23%/°C), and the calculated temperature yielding the maximum weight loss rate (340 °C) was lower than the experimental result of 346 °C.

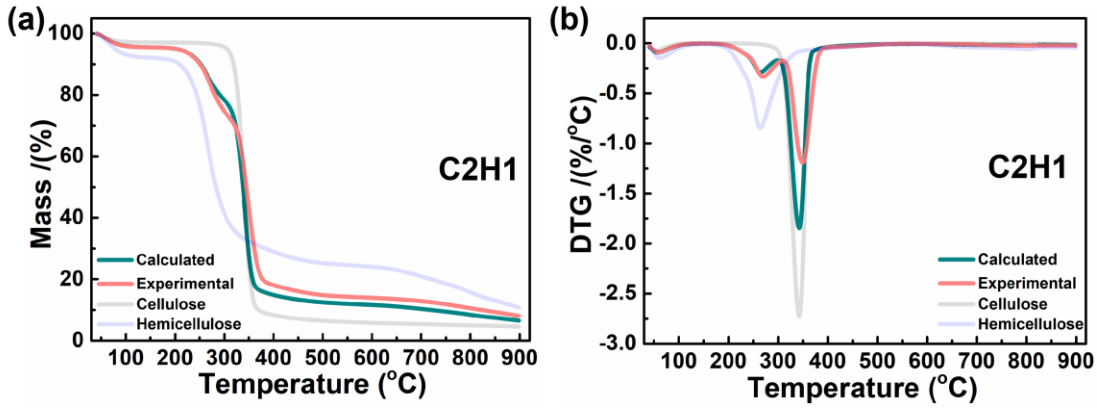

Fig. 3. Pyrolysis curves of cellulose, hemicellulose and C2H1. (a) TG, (b) DTG

The phenomena described above can be attributed to the fact that the product melted into a liquid phase during the hemicellulose pyrolysis at low temperatures. Such a liquid phase was wrapped on the surface of cellulose to inhibit its emitting of pyrolyzed volatiles, leading to an increased T_{end} for cellulose pyrolysis. It also delayed the weight loss peak of cellulose, moving it to the high temperature side and increasing the possibility of a secondary reaction (Hosoya *et al*. 2007a). In addition, most of the volatiles produced during hemicellulose pyrolysis were similar to those of cellulose, which increased the concentrations of cellulose's volatile products. This has led to a reduced weight loss rate of cellulose, and increased the solid residue (Rosillo-Calle *et al.* 2016). Overall, the

presence of hemicellulose inhibits the pyrolysis process of cellulose to some extent.

Co-pyrolysis of lignin and hemicellulose

Experimental and calculated TG and DTG curves for the mixture of lignin and hemicellulose (L2H1) are shown in Fig. 4a and 4b, respectively. Compared with the single component pyrolysis processes, there were two distinct weight loss peaks in the L2H1 DTG curve at 268 °C and 748 °C, respectively. However, there was no weight loss peak at the maximum weight loss rate of single lignin at 344 °C. The temperature of the first weight loss peak at 268 °C was basically consistent with that of single hemicellulose, and the temperature of the second one at 748 °C was fairly consistent with that of single lignin, which indicated that the first weight loss peak was dominated by hemicellulose, and the second one was dominated by lignin. No statistically significant differences were identified in the comparison of experimental versus calculated parameters for the co-pyrolysis process.

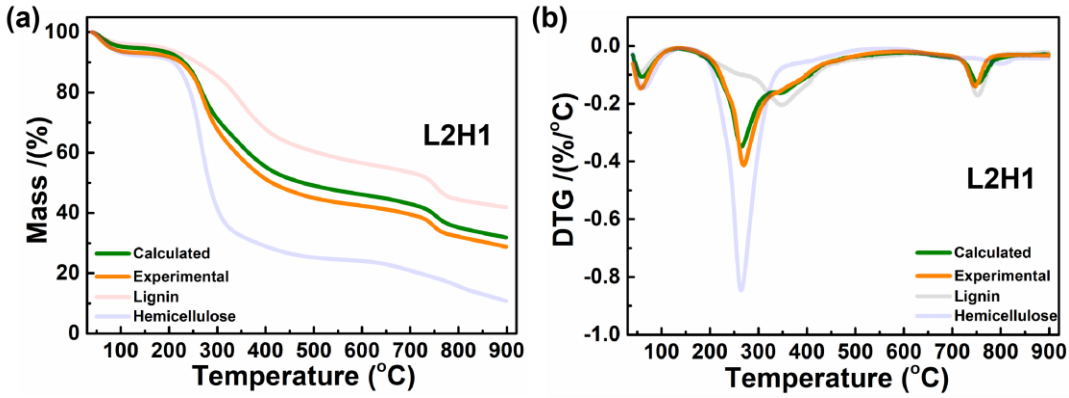

Fig. 4. Pyrolysis curves of lignin, hemicellulose and L2H1, (a) TG, (b) DTG

Co-pyrolysis of cellulose, lignin, and hemicellulose

Experimental and calculated TG and DTG curves for the mixture of cellulose, lignin, and hemicellulose (C2L2H1) are shown in Fig. 5a and 5b, respectively. There were three weight loss peaks in the co-pyrolysis of the three macromolecules, which were located at 268 °C, 347 °C, and 742 °C, respectively. According to the single component pyrolysis processes, the first weight loss peak was caused by the pyrolysis process of hemicellulose, and the second one was due to the pyrolysis of cellulose and lignin, while the third one was attributed to the pyrolysis of lignin and hemicellulose. The experimental and calculated parameters of the co-pyrolysis process also showed some discrepancies. The calculated maximum weight loss rate (1.25%/°C) was higher than the experimental result (0.92%/°C), and the calculated temperature yielding the T_{max} was lower than the experimental result.

The experimental pyrolysis residue of the C2L2H1 was lower than the calculated result. This is mainly due to the presence of hemicellulose, which increases the main pyrolysis temperature range of the mixture and shifts the maximum weight loss temperature to the high temperature side. The presence of lignin and hemicellulose greatly reduces the weight loss rate of the mixture, which is consistent with the results discussed above for binary mixtures. These observations indicate that there is a strong interaction between the macromolecules of cellulose, lignin, and hemicellulose during the co-pyrolysis process (Wang *et al*. 2008).

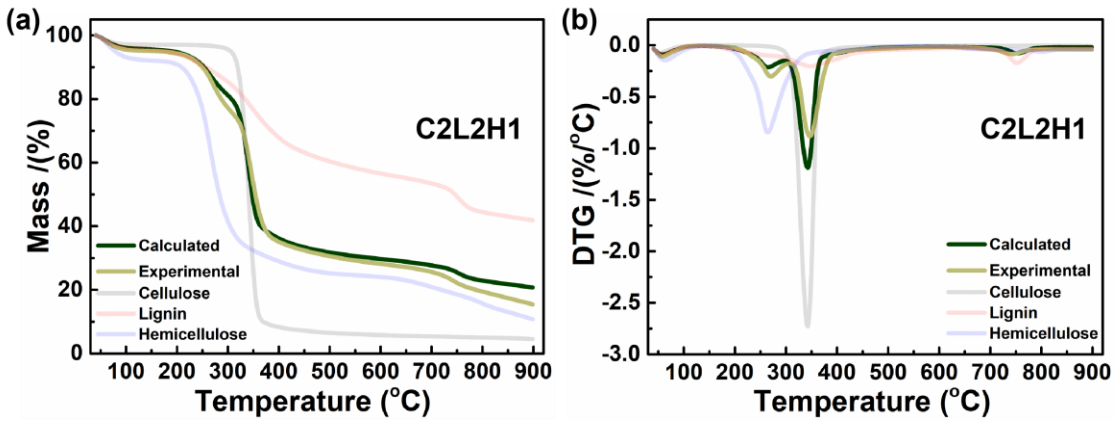

Fig. 5. Pyrolysis curves of cellulose, lignin, hemicellulose and C2L2H1. (a) TG, (b) DTG

Table 2. Parameters Related to Co-pyrolysis of Mixtures of Cellulose, Lignin, and Hemicellulose

Sample	T_{in} (°C)	T_{end} (°C)	T_{max} (°C)	DTG_{max} (%/°C)	Residue (%)
Experimental C1L1	154±51abc	792±31c	343±1bc	-1.22±0.08c	15.74±6.60b
Calculated C1L1	176±5a	746±5bc	341±1b	-1.59±0.08b	22.76±0.30c
Experimental C2H1	109±48abc	720±50b	346±2d	-1.23±0.06c	6.15±2.76a
Calculated C2H1	149±49abc	669±35a	340±1b	-1.94±0.11a	4.58±1.87a
Experimental L2H1	62±4b	782±12c	268±1a	-0.38±0.03e	30.56±1.69d
Calculated L2H1	73±5bc	786±11c	267±2a	-0.37±0.02e	32.07±1.59d
Experimental C2L2H1	84±7bc	783±22c	345±2cd	-0.92±0.07d	16.03±4.59b
Calculated C2L2H1	93±1c	757±3bc	340±1b	-1.25±0.07c	19.50±0.53c

T_{in}, the starting temperature of pyrolysis, defined as the temperature point when the total mass loss has reached 5% (Wu *et al.* 2014).
T_{end}, the end temperature of pyrolysis, defined as the temperature point when the total mass loss has reached 95% (Wu *et al*. 2014).
T_{max}, the temperature yielding the maximum weight loss rate.
Residue refers to the residual mass of the sample when the temperature has reached 900℃.
Values in the same row with different columns indicate significant difference ($P<0.05$) according to Duncan's tests.

Pyrolysis Products of Cellulose, Hemicellulose, and Lignin

Based on TG data analysis, the T_{max} of cellulose, hemicellulose, and lignin was determined first; subsequently, the volatile products of each component at their corresponding T_{max} were collected and subjected to real-time analysis via GC-MS. The mass spectra were qualitatively and quantitatively analyzed according to the National Institute of Standards and Technology (NIST) database, and the results were summarized in Table S1-3. The results in Table S1 showed that the pyrolysis products of cellulose were very complex, including sugars, esters, furans, ketones, alcohols, aldehydes, acids, and aryl compounds. This is due to the occurrence of very complex thermochemical reactions during cellulose's pyrolysis process. As shown in the product distribution chart in Fig. 6, the main products of the cellulose's pyrolysis were dehydrated sugars, accounting for about 62.2% from the relative area content analysis. These sugars were results of the cleavage of glycosidic bond and transglycosylation (Wang *et al*. 2003; Zhou 2017). The main products of hemicellulose's pyrolysis were ketones and furans (Table S2). The formation of ketones was mainly due to the cleavage of the O-glycosidic bond of the hemicellulose backbone

and the subsequent dehydroxylation reaction. In addition, compounds such as alcohols, aldehydes, and acids were also detected, and the acids may be formed by the cleavage of acetyl groups in hemicellulose molecules (Abbasi and Abbasi 2010; Patwardhan *et al*. 2011). Lastly, the pyrolysis of lignin mainly produced aryl compounds, inorganic gases, furans, and other varieties of compounds. Among these products, the dominant ones were phenol, 2-methoxy-, SO_2, vanillin, and dimethyl sulfide, with their relative area contents of 40.2%, 26.0%, 7.38%, and 4.15%, respectively. Lignin is a disordered polymer formed by three phenylpropane units linked by a variety of alkyl ether bonds, and the cleavage of alkyl and aryl ether bonds occurs when heated at high temperatures, resulting in a variety of complex phenolic compounds (Gooty *et al*. 2014; Custodis *et al*. 2015).

Combined with the above analysis and previous works (Alén *et al.* 1996; Collard and Blin 2014), at relatively low pyrolysis temperatures (below 300 °C), small-molecule ketones, acids, furans, and aldehydes are the primary products. When the pyrolysis temperature increases to a higher range, the pyrolysis products are dominated by ketones, esters, and saccharide. These compounds are mainly generated from the cleavage of glycosidic bonds in cellulose and the production of large amounts of anhydrosugars through transglycosylation. Notably, across the entire temperature spectrum, aryl compounds were consistently present. This phenomenon is primarily ascribed to the slow pyrolysis process that lignin undergoes throughout all temperature ranges: specifically, the cleavage of carbon-oxygen bridges and carbon-carbon bonds between aromatic rings results in the release of aryl compounds and small-molecule compounds. When the temperature reaches an elevated level (above 600 °C), it triggers the secondary pyrolysis of residual cellulose, lignin, and hemicellulose, further leading to the release of small-molecule gases and aryl compounds.

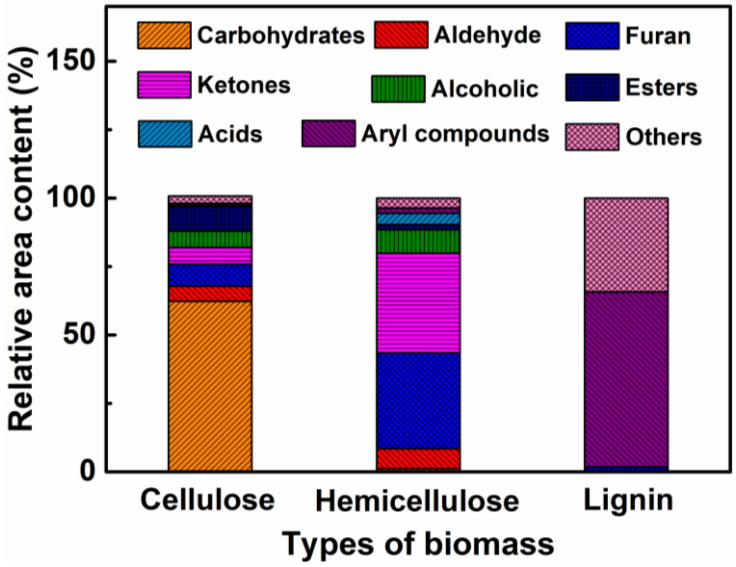

Fig. 6. Distribution chart of pyrolysis products of the three biomass components

Effect of Mixture of Cellulose, Hemicellulose, and Lignin on Pyrolysis Product

Effect of mixture of cellulose and lignin on pyrolysis products

Based on the above analysis in Fig. 6, it was found that the pyrolysis of single-component cellulose produced 97.4% non-aryl compounds, and the pyrolysis of single-component lignin produced 64.0% aryl compounds. Therefore, the non-aryl compounds produced during the co-pyrolysis of cellulose and lignin were mainly derived from cellulose, while the aryl compounds mainly originated from lignin.

The experimental contents of the non-aryl compounds produced by the pyrolysis of C1L1 were higher than the calculated results (Fig. 7 and Table S4), and the experimental relative contents of sugars, esters, and alcohols were lower than the calculated results. These results indicate that the presence of lignin inhibited the pyrolysis of cellulose to produce sugars and esters, which is consistent with the results of Zhu *et al*. (2016). However, the experimental relative contents of aldehydes, furans, ketones, and acids were higher than the calculated results, indicating that the presence of lignin promoted the pyrolysis of cellulose to produce aldehydes, furans, ketones, and acids. For the aryl compounds, the experimental content produced by the co-pyrolysis of C1L1 was lower than the calculated value, indicating that co-pyrolysis inhibited the formation of aryl compounds (Norinaga *et al*. 2014).

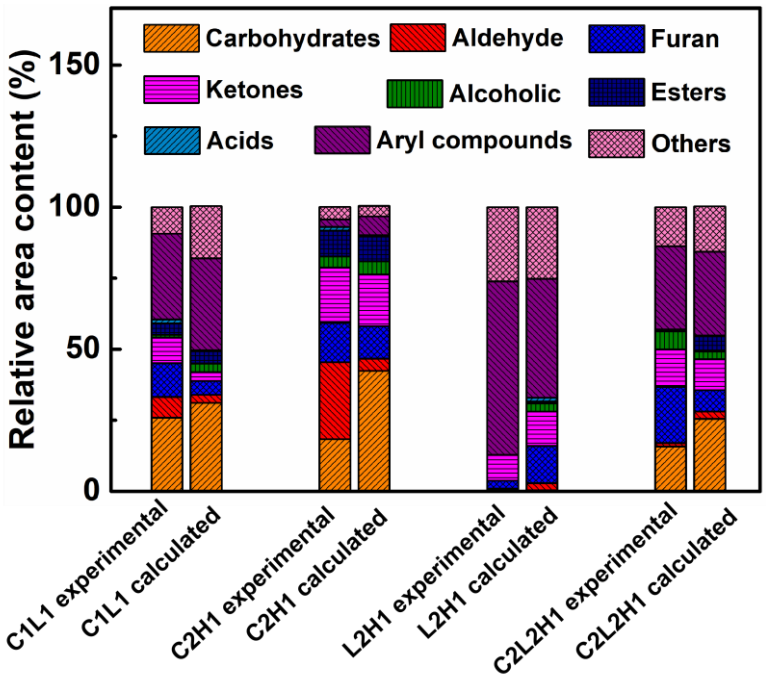

Fig. 7. Distribution of co-pyrolysis products of three biomass components

Effect of mixture of cellulose and hemicellulose on pyrolysis products

As both cellulose and hemicellulose belong to the polysaccharide category, the co-pyrolysis of C2H1 yielded fewer aryl compounds (2.69%, Table S5). This is much lower than that of the aryl compounds produced by the pyrolysis of single-component hemicellulose (18.33%, Table S6). Moreover, the experimental aryl compounds content produced by co-pyrolysis of C2H1 was lower than the calculated result (Fig. 7 and Table S5), indicating that the presence of cellulose inhibited the pyrolysis of hemicellulose to

produce aryl compounds. The experimental relative contents of sugars and alcohols were also lower than the calculated values. Specifically, the experimental relative content of sugars (18.31%) was much lower than its calculated value (42.38%). This result indicates that the presence of hemicellulose significantly inhibited the pyrolysis of cellulose to produce sugars and esters, which was consistent with the results of Li *et al*. (2015). The experimental contents of aldehydes, furans, ketones, esters, and acids were higher than the calculated values. The difference between the experimental (27.09%) and calculated contents (4.28%) of aldehyde compounds was substantial, and the differences in others were small. These observations indicate that the presence of hemicellulose promoted the pyrolysis of cellulose to produce aldehydes, furans, ketones, esters, and acids. For the aryl compounds, the experimental content produced by co-pyrolysis of C1L1 was lower than the calculated value, indicating that co-pyrolysis inhibited the formation of aryl compounds.

Effect of mixture of lignin and hemicellulose on pyrolysis products

As shown in Fig. 6, the pyrolysis of single-component lignin produced 64.0% aryl compounds, while the pyrolysis of single-component hemicellulose produced 98.1% non-aryl compounds. Therefore, the non-aryl compounds produced during the co-pyrolysis of lignin and hemicellulose were mainly derived from hemicellulose, whereas the aryl compounds mainly originated from lignin. The experimental contents of the non-aryl compounds produced by the co-pyrolysis of L2H1 were lower than the calculated results (Fig. 7, Tables S7 and S8), among which the experimental relative contents of aldehydes, furans, ketones, esters, acids, and alcohols were all lower than the calculated values. The difference between the experimental content (2.73%) and the calculated result (13.1%) of furans was substantial, while the differences in others were small. These observations indicate that the presence of lignin inhibited the pyrolysis of hemicellulose to produce aldehydes, furans, ketones, esters, acids, and alcohols, which was consistent with the results of Liu *et al.* (2017). For the aryl compounds, the experimental relative content (61.1%) produced by the co-pyrolysis of L2H1 was higher than the calculated result (41.9%), indicating that the presence of hemicellulose inhibited the pyrolysis of lignin to produce aryl compounds.

Effect of mixture of cellulose, lignin, and hemicellulose on the pyrolysis products

As depicted in Fig. 6, the pyrolysis of cellulose as a single component yielded 97.4% non-aryl compounds, while the pyrolysis of lignin alone produced 64.0% aryl compounds, and hemicellulose pyrolyzed in isolation generated 98.1% non-aryl compounds. This result explicitly demonstrates that during the co-pyrolysis of cellulose, lignin, and hemicellulose, cellulose and hemicellulose serve as the primary sources of non-aryl compounds, whereas aryl compounds are predominantly derived from lignin. This finding establishes a fundamental basis for identifying pyrolysis product origins, which is essential for the subsequent investigation of inter-component interactions.

With specific regard to aryl compounds-recognized as the characteristic products of lignin pyrolysis-the experimental relative content of aryl compounds in the C2L2H1 co-pyrolysis system was 29.3% (see Fig. 7 and Table S9), which was marginally lower than the calculated value of 29.5%. This observation implies that the concurrent presence of hemicellulose and cellulose may exert a weak inhibitory effect on the formation of aryl compounds during lignin pyrolysis. For the subcategories of non-aryl compounds, the experimental relative contents of saccharides, aldehydes, and esters were all lower than their respective theoretical values. Among these, the discrepancy between the experimental

value (0.01%) and theoretical value (5.29%) of esters was the most prominent. This phenomenon aligns with the aforementioned findings from the C1L1 and L2H1 systems, confirming that the presence of lignin can suppress the formation of esters during the co-pyrolysis of cellulose and hemicellulose. Additionally, the difference between the experimental value (15.7%) and theoretical value (25.4%) of saccharides was also highly significant. Notably, the experimental relative contents of furans, alcohols, ketones, and acids were all higher than their corresponding theoretical values. Among these, the discrepancy between the experimental value (19.8%) and theoretical value (7.55%) of furans was the most striking. This differential outcome indicates that lignin exerts a promotional effect on the generation of the aforementioned four compound classes. The underlying mechanism can be attributed to the dehydration and polymerization reactions that occur between the pyrolysis products of lignin (*e.g.*, phenols) and the pyrolysis intermediates of cellulose/hemicellulose (*e.g.*, dehydrated sugars, small-molecule aldehydes) during the co-pyrolysis of the three components, which in turn leads to the formation of more carbonyl-containing compounds such as furans and ketones (Collard and Blin 2014).

CONCLUSIONS

Using thermogravimetry – gas chromatography/mass spectrometry (TG-GC/MS) hyphenated technology, this study systematically investigated the individual and co-pyrolysis characteristics of the three core components of biomass (cellulose, hemicellulose, and lignin), and in-depth analyzed the regulatory mechanism of interactions between components on pyrolysis behavior and product distribution. The main conclusions are as follows.

1. The intrinsic differences in the individual pyrolysis behaviors of the three components were clarified, and these differences originate from the inherent chemical structural characteristics of the three components. More importantly, through the comparative analysis between experimental values and theoretical superimposed values (based on Eq. 1), the specific interactions during co-pyrolysis of different component combinations were verified. These quantitative analysis results provide data support for deciphering the pyrolysis mechanism of real biomass.
2. The characteristic product profiles of the three components during individual pyrolysis were identified: cellulose was dominated by anhydrosugars; hemicellulose was centered on ketones and furans; and lignin was rich in aryl compounds. Further research revealed that the co-pyrolysis process exerts an influential impact on the distribution of its products, including sugars, aldehydes, furans, ketones, alcohols, esters, acids, and aryl compounds.

In summary, by revealing the co-pyrolysis interactions of biomass components and the distribution mechanism of pyrolysis products, this study not only deepens the understanding of the intrinsic nature of biomass pyrolysis, but it also provides key theoretical basis and practical guidance for the high-value application of biomass pyrolysis technology.

ACKNOWLEDGMENTS

This work was supported by Central Public-interest Scientific Institution Basal Research Fund (1610232023020), Natural Science Foundation of Shandong Province (ZR2023QC207), Natural Science Foundation of Qingdao City (23-2-1-52-zyyd-jch), Science and Technology Major Project of China National Tobacco Corporation (110202501012(SZ-04)), Science and Technology Project of Beijing Life Science Academy Company Limited (2023000CC0090), Science and Technology Project of Hunan Tobacco Company Chenzhou Company (CZYC2023JS05), Science and Technology Project of China Tobacco Shandong Industrial Company Limited (2024370000340436).

Authorship Contribution Statement

Kun Wang: Conceptualization, Methodology, Validation, Writing-original draft preparation. **Xinhua Song**: Data curation, Supervision, Resources. **Hongxiao Yu**: Writing-review and editing. **Tongxu Cui**: Software, Visualization. **Jian Liu**: Formal analysis. **Zelin He**: Formal analysis. **Mengying Chen**: Visualization. **Binbin Yao**: Investigation.

Declaration of Competing Interest

The authors declare that they have no known competing financial interests or personal relationships that could have appeared to influence the work reported in this paper.

REFERENCES CITED

Abbasi, T., and Abbasi, S. A. (2010). "Biomass energy and the environmental impacts associated with its production and utilization," *Renewable Sustainable Energy Rev.* 14 (3), 919-937. https://doi.org/10.1016/j.rser.2009.11.006

Alen, R., Kouppala, E., and Oesch, P. (1996). "Formation of the main degradation compound groups from wood and its components during pyrolysis," *J. Anal. Appl. Pyrol.* 36, 137-148. https://doi.org/10.1016/0165-2370(96)00932-1

Argyropoulos, D. S., Jurasek, L., Kristofová, L., Xia, Z., Sun, Y., and Palus, E. E. (2002). "Abundance and reactivity of dibenzodioxocins in softwood lignin," *J. Agric. Food. Chem.* 4, 658-66. https://doi.org/10.1021/jf010909g

Ball, R., McIntosh, A. C., and Brindley, J. (2004). "Feedback processes in cellulose thermal decomposition: implications for fire-retarding strategies and treatments," *Combust. Theory Modelling* 8(2), 281-291. https://doi.org/10.1088/1364-7830/8/2/005

Bowden, P. J. (1984). "Comparison of three routine oven methods for grain moisture content determination," *J. stored Prod. Res.* 20(2), 97-106. https://doi.org/10.1016/0022-474x(84)90015-8

Brunner, P. H., and Roberts, P. V. (1980). "The significance of heating rate on char yield and char properties in the pyrolysis of cellulose," *Carbon* 18(3), 217-224. https://doi.org/10.1016/0008-6223(80)90064-0

Collard, F., and Blin, J. (2014). "A review on pyrolysis of biomass constituents: Mechanisms and composition of the products obtained from the conversion of cellulose, hemicelluloses and lignin," *Renewable Sustainable Energy Rev.* 38, 594-

608. https://doi.org/10.1016/j.rser.2014.06.013

Custodis, V. B. F., Christian, B., Frédéric, V., and Bokhoven, J. A. (2015). "Phenols and aromatics from fast pyrolysis of variously prepared lignins from hard- and softwoods," *J. Anal. Appl. Pyrol.* 115, 214-223. https://doi.org/10.1016/j.jaap.2015.07.018

Dorez, G., Ferry, L., Sonnier, R., Taguet, A., and Lopez-Cuesta, J. M. (2014). "Effect of cellulose, hemicellulose and lignin contents on pyrolysis and combustion of natural fibers," *J. Anal. Appl. Pyrol.* 107, 323-331. https://doi.org/10.1016/j.jaap.2014.03.017

Etale, A., Onyianta, A. J., Turner, S. R., and Eichhorn, S. J. (2023). "Cellulose: A review of water interactions, applications in composites, and water treatment," *Chem. Rev.* 123 (5), 2016-2048. https://doi.org/10.1021/acs.chemrev.2c00477

Gooty, A. T., Li, D., Berruti, F., and Briens, C. (2014). "Kraft-lignin pyrolysis and fractional condensation of its bio-oil vapors," *J. Anal. Appl. Pyrol.* 106, 33-40. https://doi.org/10.1016/j.jaap.2013.12.006

Guo, R., Yin, S. S., and Francis, T. S. (2007). "Photonic fiber and crystal devices: Advances in materials and innovations in device applications," *Photonic Fiber and Crystal Devices: Advances in Materials and Innovations in Device Applications*, 6698.

Hosoya, T., Kawamoto, H., and Saka, S. (2007a). "Cellulose–hemicellulose and cellulose–lignin interactions in wood pyrolysis at gasification temperature," *J. Anal. Appl. Pyrol*. 80 (1), 118-125. https://doi.org/10.1016/j.jaap.2007.01.006

Hosoya, T., Kawamoto, H., and Saka, S. (2007b). "Pyrolysis behaviors of wood and its constituent polymers at gasification temperature," *J. Anal. Appl. Pyrol.* 78 (2), 328-336. https://doi.org/10.1016/j.jaap.2006.08.008

Inaba, K., and Matsumoto, K. (1999). "The development of the measurement of particle concentration using a commercial laser diffraction particle size analyzer," *Advanced Powder Technol.* 10(1), 89-103. https://doi.org/10.1016/S0921-8831(08)60459-8

Jin, W., Shen, D., Liu, Q., and Xiao, R. (2016). "Evaluation of the co-pyrolysis of lignin with plastic polymers by TG-FTIR and Py-GC/MS," *Polym. Degrad. Stabil.* 133, 65-74. https://doi.org/10.1016/j.polymdegradstab.2016.08.001

Kim, L., Hwang, H., Park, J., Oh, S., and Choi, J. (2014). "Predicting structural change of lignin macromolecules before and after heat treatment using the pyrolysis-GC/MS technique," *J. Anal. Appl. Pyrol.* 110, 305-312. https://doi.org/10.1016/j.jaap.2014.09.020

Kuroda, K. I., Inoue, Y., and Sakai, K. (1990). "Analysis of lignin by pyrolysis-gas chromatography. I. Effect of inorganic substances on guaiacol-derivative yield from softwoods and their lignins," *J. Anal. Appl. Pyrol.* 18(1), 59-69. https://doi.org/10.1016/0165-2370(90)85005-8

Lavarack, B. P., Griffin, G. J., and Rodman, D. (2002). "The acid hydrolysis of sugarcane bagasse hemicellulose to produce xylose, arabinose, glucose and other products," *Biomass Bioenergy* 23(5), 367-380. https://doi.org/10.1016/S0961-9534(02)00066-1

Lédé, J., Blanchard, F., and Boutin, O. (2002). "Radiant flash pyrolysis of cellulose pellets: products and mechanisms involved in transient and steady state conditions," *Fuel* 81(10), 1269-1279. https://doi.org/10.1016/S0016-2361(02)00039-X

Li, C., Sun, Y., Dong, D., Gao, G., Zhang, S., Wang, Y., Xiang, J., Hu, S., Mortaza, G., and Hu, X. (2021). "Co-pyrolysis of cellulose/lignin and sawdust: Influence of secondary condensation of the volatiles on characteristics of biochar," *Energy* 226, article 120442. https://doi.org/10.1016/j.energy.2021.120442

Li, X., Jiao, L., Fan, Y., Chen, L., and Cai, Y. (2015). "Effects of cellulose, xylan and lignin content on biomass pyrolysis characteristics and product distribution," *Trans. Chin. Soc. Agric. Eng.* 31(13), 236-243. https://doi.org/10.11975/j.issn.1002-6819.2015.13.033

Liu, J., Hou, Q., Ju, M., Ji, P., Sun, Q., and Li, W. (2020). "Biomass pyrolysis technology by catalytic fast, pyrolysis, catalytic co-pyrolysis and microwave-assisted pyrolysis: A review," *Catalysts* 10, article 742. https://doi.org/10.3390/catal10070742

Liu, E., Guo, Z., Wang, Y., Wei, X., and Li, M. (2024). "Biomass analysis of resource utilization system," *Biomass Analysis of Resource Utilization System THERMAL SCIENCE* 28(3A), 2093-2100. https://doi.org/10.2298/TSCI2403093L

Liu, Q., Wang, S., Zheng, Y., Luo, Z., and Cen, K. (2008). "Mechanism study of wood lignin pyrolysis by using TG–FTIR analysis," *J. Anal. Appl. Pyrol.* 82(1), 170-177. https://doi.org/10.1016/j.jaap.2008.03.007

Liu, Q., Zhong, Z., Wang, S., and Luo, Z. (2011). "Interactions of biomass components during pyrolysis: A TG-FTIR study," *J. Anal. Appl. Pyrol.* 90(2), 213-218. https://doi.org/10.1016/j.jaap.2010.12.009

Liu, Z, Wang, L., Zhang, Y., Li, Y., Li, Z., and Cai, H. (2017). "Cellulose-lignin and xylan-lignin interactions on the formation of lignin-derived phenols in pyrolysis oil," *BioResources* 12(3), 4958-4971. https://doi.org/10.15376/biores.12.3.4958-4971

Lu, Q., Yang, X.C., Dong, C.Q., Zhang, Z.F., Zhang, X.M., and Zhu, X.F. (2011). "Influence of pyrolysis temperature and time on the cellulose fast pyrolysis products: Analytical Py-GC/MS study," *J. Anal. Appl. Pyrol.* 92(2), 430-438. https://doi.org/10.1016/j.jaap.2011.08.006

Marchessault, R. H., and Sundararajan, P. R. (1983). "2-Cellulose," *The Polysaccharides*, 11-95. https://doi.org/10.1016/B978-0-12-065602-8.50007-8

McKendry, P. (2002). "Energy production from biomass (part 1): Overview of biomass," *Bioresource Technol.* 83(1), 37-46. https://doi.org/10.1016/S0960-8524(01)00118-3

Norinaga, K., Yang, H., Tanaka, R., Appari, S., Iwanaga, K., Takashima, Y., Kudo, S., Shoji, T., and Hayashi, J. I. (2014). "A mechanistic study on the reaction pathways leading to benzene and naphthalene in cellulose vapor phase cracking," *Biomass and Bioenergy* 69, 144-154. https://doi.org/10.1016/j.biombioe.2014.07.008

Parthasarathi, R., Romero, R. A., Redondo, A., and Gnanakaran, S. (2011). "Theoretical study of the remarkably diverse linkages in lignin," *J. Phys. Chem. Lett.* 2 (20), 2660-2666. https://doi.org/10.1021/jz201201q

Patwardhan, P. R., Brown, R. C., and Shanks, B. H. (2011). "Product distribution from the fast pyrolysis of hemicellulose," *ChemSusChem* 4(5), 636-643. https://doi.org/10.1002/cssc.201000425

Rosillo-Calle, F. (2016). "A review of biomass energy–shortcomings and concerns," *J. Chem. Technol. Biot.* 91(7), 1933-1945. https://doi.org/10.1002/jctb.4918

Saura-Calixto, F. S., Cañellas, J., and Garcia-Raso, J. (1983). "Determination of hemicellulose, cellulose and lignin contents of dietary fibre and crude fibre of several seed hulls. Data comparison," *Z. Lebensm. Unters. Forch.* 177, 200-202. https://doi.org/10.1007/BF01146796

Shafizadeh, F., and Fu, Y. L. (1973). "Pyrolysis of cellulose," *Carbohyd. Res.* 29(1), 113-122. https://doi.org/10.1016/S0008-6215(00)82074-1

Shen, D., Gu, S., and Bridgwater, A. V. (2010). "The thermal performance of the polysaccharides extracted from hardwood: Cellulose and hemicellulose," *Carbohydr. Chem.* 82 (1), 39-45. https://doi.org/10.1016/j.carbpol.2010.04.018

Stefanidis, S. D., Kalogiannis, K. G., Iliopoulou, E. F., Michailof, C. M., Pilavachi, P. A., and Lappas. (2014). "A study of lignocellulosic biomass pyrolysis via the pyrolysis of cellulose, hemicellulose and lignin," *J. Anal. Appl. Pyrol.* 105, 143-150. https://doi.org/10.1016/j.jaap.2013.10.013

Wang, G., Li, W., Li, B., and Chen, H. (2008). "TG study on pyrolysis of biomass and its three components under syngas," *Fuel* 87(4-5), 552-558. https://doi.org/10.1016/j.fuel.2007.02.032

Wang, S., Gu, x., Wang, K., and Luo, Z. (2011). "Influence of the interaction of components on the pyrolysis behavior of biomass," *J. Anal. Appl. Pyrol.* 91(1), 183-189. https://doi.org/10.1016/j.jaap.2011.02.006

Wang, S., Liao, Y., Tan, H., Luo, Z., and Cen, K. (2003). "Mechanism of cellulose rapid pyrolysis. II. Mechanism analysis," *J. Fuel. Chem. Technol.* (04), 317-321. https://doi.org/10.1021/ie030774z

Weng, S., Deng, M., Chen, S., Yang, R., Li, J., Zhao, X., and Zhang, W. (2024). "Application of pectin hydrolyzing bacteria in tobacco to improve flue-cured tobacco quality," *Front. Bioeng. Biotech.* 2024, article 1340160. https://doi.org/10.3389/fbioe.2024.1340160

Wu, K., Yang, K., Zhu, Y., Luo, B., Chu, C., Li, M., Zhang, Y., and Zhang, H. (2023). "The co-pyrolysis interactionsof isolated lignins and cellulose by experiments and theoretical calculations," *Energy* 263(PC), article 125811. https://doi.org/10.1016/j.energy.2022.125811

Wu, S., Shen, D., Hu, J., Zhang, H., and Xiao, R. (2014). "Intensive interaction region during co-pyrolysis of lignin and cellulose: Experimental observation and kinetic assessment," *BioResources* 9(2), 2259-2273. https://doi.org/10.15376/biores.9.2.2259-2273

Wu, S., Shen, D., Hu, J., Zhang, H., and Xiao, R. (2016a). "Cellulose-hemicellulose interactions during fast pyrolysis with different temperatures and mixing methods," *Biomass Bioenergy* 95, 55-63. https://doi.org/10.1016/j.biombioe.2016.09.015

Wu, S., Shen, D., Hu, J., Zhang, H., and Xiao, R. (2016b). "Cellulose-lignin interactions during fast pyrolysis with different temperatures and mixing methods," *Biomass and Bioenergy* 90, 209-217. DOI: 10.1016/j.biombioe.2016.04.012

Yang, H., Yan, R., Chen, H., Zheng, C., Lee, D., and David, T. L. (2006). "In-depth investigation of biomass pyrolysis based on three major components hemicellulose, cellulose and lignin," *Energy Fuels* 20(1), 388-393. https://doi.org/10.1021/ef0580117

Yang, H., Yan, R., Chen, H., Zheng, C., Lee, D., and Zheng, C. (2007). "Characteristics of hemicellulose, cellulose and lignin pyrolysis," *Fuel* 86, 1781-1788. https://doi.org/10.1016/j.fuel.2006.12.013

Ye, X., Lu, Q., Jiang, X., Wang, X., Hu, B., Li, W., and Dong, C. (2017). "The co-pyrolysis interactions of isolated lignins and cellulose by experiments and theoretical calculations," *J. Therm. Anal. Calorim.* 130, 975-984. https://doi.org/10.1007/s10973-017-6465-3

Zhang, C., Chao, L., Zhang, Z., Zhang, Z., Zhan, L., and Li, Q. (2021). "Pyrolysis of cellulose: Evolution of functionalities and structure of bio-char versus temperature," *Renewable Sustainable Energy Rev.* 2021, article 135110416. https://doi.org/10.1016/j.rser.2020.110416

Zhang, J., Toghiani, H., Mohan, D., Charles, U. P., and Rebecca, K. T. (2007). "Product analysis and thermodynamic simulations from the pyrolysis of several biomass

feedstocks," *Energy Fuels* 21(4), 2373-2385. https://doi.org/10.1021/ef0606557

Zhou, W. (2017). *Study on Pyrolysis of Lignocellulosic Biomass and Product Analysis*, Master's Thesis, Tianjin University of Technology, Tianjin, China.

Zhu, L., Zhong, Z., Wang, H., and Wang, Z. (2016). "Simulation of large biomass pellets in fluidized bed by DEM-CFD," *Korean J. Chem. Eng.* 33(10), 3021-3028. https://doi.org/10.1007/s11814-016-0167-6

Article submitted: March 24, 2025; Peer review completed: September 16, 2025; Revised version received: October 15, 2205; Accepted: March 4, 2026; Published: March 27, 2026.
DOI: 10.15376/biores.21.2.4207-4234

APPENDIX

Table S1. Volatile Pyrolysis Products of Cellulose at Maximum Weight Loss Temperature

NO.	RT/min	Name	CAS number	Relative peak area/%
1	1.99	Glyoxal	107-22-2	0.32
2	2.07	Furan	110-00-9	1.55
3	2.41	1,4-Pentadien-3-one	1890-28-4	2.79
4	2.77	Furan, 2,3-dihydro-	1191-99-7	0.14
5	3.03	4-Heptanol	589-55-9	0.14
6	3.30	Furan, 2,5-dimethyl-	625-86-5	0.18
7	3.54	2-Vinylfuran	1487-18-9	0.18
8	4.06	3,4-Pentadienal	4009-55-6	0.47
9	4.48	2(5H)-Furanone	497-23-4	0.28
10	5.09	Carbonocyanidic acid, ethyl ester	623-49-4	5.49
11	5.58	3-Furaldehyde	498-60-2	0.35
12	6.14	Furfural	98-01-1	4.40
13	6.39	2-Amino-1,3,5-triazine	4122-04-7	0.49
14	6.94	2-Furanmethanol	98-00-0	0.20
15	7.35	Furan, 2-propyl-	4229-91-8	1.09
16	7.99	4-Cyclopentene-1,3-dione	930-60-9	0.19
17	8.18	1-Propanone, 1-(2-furanyl)-	3194-15-8	0.22
18	9.17	Ethanone,1-(2-furanyl)-	1192-62-7	0.71
19	9.76	6-Oxa-bicyclo[3.1.0]hexan-3-one	74017-10-0	0.31
20	10.42	2(5H)-Furanone, 5-methyl-	591-11-7	0.13
21	10.56	2,5-Furandione, dihydro-3-methylene-	2170-03-8	0.19
22	10.70	2-Cyclohexen-1-one	930-68-7	0.16
23	11.07	Hydroquinone	123-31-9	0.13
24	11.52	2-Furancarboxaldehyde, 5-methyl-	620-02-0	1.00
25	12.18	1-Propanone, 1-(2-furanyl)-	3194-15-8	0.30
26	12.52	Resorcinol	108-46-3	0.32
27	13.32	N-Butyl-tert-butylamine	16486-74-1	0.57
28	14.35	4H-1,2,4-Triazole, 3,4,5-trimethyl-	16759-45-8	0.24
29	14.60	Maleic hydrazide	123-33-1	0.09
30	15.20	1-Benzofuran-5-ol	13196-10-6	0.10
31	15.39	3-Cyclopropyl-3-oxopropanenitrile	118431-88-2	0.12
32	15.86	1,3-Dioxolan-2-one, 4,4,5,5-tetramethyl-	19424-29-4	0.21
33	16.81	1,2-Hexadiene, 5-methyl-	13865-36-6	0.18
34	17.05	3-Furancarboxylic acid, methyl ester	13129-23-2	0.11
35	17.13	Orcinol	504-15-4	0.16
36	17.27	2-Octen-1-ol, (Z)-	26001-58-1	0.19
37	17.35	Furyl hydroxymethyl ketone	17678-19-2	0.20
38	17.54	Furaneol	3658-77-3	0.18
39	18.11	Tiglic acid	80-59-1	0.49
40	18.69	Levoglucosenone	37112-31-5	12.79
41	22.35	4-Methyl-2-oxopentanenitrile	66582-16-9	2.18

42	22.93	2-Butene-1,4-diol, (Z)-	6117-80-2	0.25
43	23.64	1,4:3,6-Dianhydro-α-d-glucopyranose	~	4.77
44	24.32	5-Hydroxymethylfurfural	67-47-0	1.64
45	24.99	cis-1,2-Cyclohexanediol	1792-81-0	1.19
46	30.86	1-Naphthalenol, 1,2,3,4,4a,7,8,8a-octahydro-1,6-dimethyl-4-(1-methylethyl)-, [1R-(1α,4β,4aβ,8aβ)]-	19435-97-3	4.02
47	34.09	Pentanoic acid, 2,2,4-trimethyl-3-carboxyisopropyl, isobutyl ester	~	3.44
48	34.92	Benzophenone	119-61-9	0.70
49	37.81	β-D-Glucopyranose, 1,6-anhydro-	498-07-7	44.69
50	42.76	9H-Fluorene, 9-methylene-	4425-82-5	0.13
51	42.98	cyclohexane, 1,1'-[1,2-ethenediyl]bis-	~	0.35

Table S2. Volatile Pyrolysis Products of Hemicellulose at Maximum Weight Loss Temperature

No.	RT/min	Name	CAS number	Relative peak area/%
1	2.00	Glyoxal	107-22-2	1.42
2	2.06	Acetic acid, cyano-, 2-methoxyethyl ester	10258-54-5	2.99
3	2.35	(R)-(-)-Leucinol	53448-09-2	8.59
4	2.43	Furan, 2-methyl-	534-22-5	8.61
5	2.83	1,3-Cyclohexadiene	592-57-4	8.47
6	2.99	Propanoic acid	79-09-4	1.00
7	3.17	3-Hexanone	589-38-8	0.75
8	3.32	Furan, 2,5-dimethyl-	625-86-5	1.86
9	3.87	2,2'-Bifuran, 2,2',5,5'-tetrahydro-	98869-92-2	1.44
10	4.09	2-Butenal, 2-methyl-	1115-11-3	1.66
11	4.36	Cyclobutene, 2-propenylidene-	52097-85-5	3.09
12	4.65	Succindialdehyde	638-37-9	2.41
13	5.19	Carbonocyanidic acid, ethyl ester	623-49-4	1.38
14	5.64	Furfural	98-01-1	1.07
15	6.18	2-Cyclopenten-1-one	930-30-3	4.49
16	6.92	2-Furanmethanol	98-00-0	7.04
17	7.48	2-Propanone, 1-(acetyloxy)-	592-20-1	1.24
18	8.02	4-Cyclopentene-1,3-dione	930-60-9	1.14
19	8.38	2-Cyclopenten-1-one, 3-ethyl-	5682-69-9	0.21
20	8.99	2-Cyclopenten-1-one, 2-methyl-	1120-73-6	0.77
21	9.10	2(5H)-Furanone	497-23-4	6.25
22	9.51	Levoglucosenone	37112-31-5	1.09
23	9.73	2-Cyclopenten-1-one, 2-hydroxy-	10493-98-8	9.61
24	11.58	2-Furancarboxaldehyde, 5-methyl-	620-02-0	0.71
25	11.81	2-Butenal, 2-ethenyl-	20521-42-0	0.52
26	12.26	2(5H)-Furanone, 3-methyl-	22122-36-7	0.63
27	12.55	Cyclohexanone, 4-methylidene-	29648-66-6	0.40
28	13.28	Cyclohexanone, 3-methyl-	591-24-2	1.76
29	14.56	1,2-Cyclopentanedione, 3-methyl-	765-70-8	1.40

30	15.18	2-Cyclopenten-1-one, 2,3-dimethyl-	1121-05-7	0.22
31	15.75	Pyrrolidine, 1-methyl-	120-94-5	0.55
32	16.06	Phenol, 3-methyl-	108-39-4	0.35
33	16.50	1H-Pyrazole-4-carboxylic acid	~	0.13
34	17.53	2-Methyl-4-octenal	30390-58-0	0.33
35	17.84	Cyclohexanone, 4-hydroxy-	13482-22-9	14.39
36	18.81	Maltol	118-71-8	0.53
37	19.62	2(3H)-Furanone, 5-butyldihydro-	104-50-7	0.51
38	22.92	Catechol	120-80-9	0.46
39	40.84	Phenol, 3,5-bis(1,1-dimethylethyl)-	1138-52-9	0.51

Table S3. Volatile Pyrolysis Products of Lignin at Maximum Weight Loss Temperature

NO.	RT/min	Name	CAS number	Relative peak area/%
1	1.99	Sulfur dioxide	7446-09-5	26.02
2	2.15	Dimethyl sulfide	75-18-3	4.15
3	2.46	Furan, 2-methyl-	534-22-5	1.79
4	3.94	Disulfide, dimethyl	624-92-0	0.72
5	4.35	Toluene	108-88-3	0.19
6	11.83	Dimethyl trisulfide	3658-80-8	0.28
7	12.48	Phenol	108-95-2	1.84
8	14.41	Benzene, 1-methoxy-4-methyl-	104-93-8	0.45
9	14.63	p-Cymene	99-87-6	0.55
10	17.16	p-Cresol	106-44-5	0.55
11	17.59	Phenol, 2-methoxy-	90-05-1	40.23
12	20.54	Benzene, 1,2-dimethoxy-	91-16-7	2.11
13	21.97	2-Methoxy-6-methylphenol	2896-67-5	0.93
14	22.39	Creosol	93-51-6	0.56
15	24.91	3,4-Dimethoxytoluene	494-99-5	2.42
16	26.54	Phenol, 4-ethyl-2-methoxy-	2785-89-9	3.09
17	28.17	2-Methoxy-4-vinylphenol	7786-61-0	2.34
18	28.68	Benzene, 4-ethyl-1,2-dimethoxy-	5888-51-7	0.63
19	29.8	Phenol, 2,6-dimethoxy-	91-10-1	0.53
20	30.62	Benzene, 4-ethenyl-1,2-dimethoxy-	6380-23-0	0.59
21	31.8	Vanillin	121-33-5	7.38
22	34.05	Phenol, 2-methoxy-4-(1-propenyl)-	97-54-1	1.15
23	35.4	Apocynin	498-02-2	1.04
24	36.06	Benzene, 1,2-dimethoxy-4-(1-propenyl)-, (E)-	6379-72-2	0.48

Table S4. Volatile Pyrolysis Products of C1L1 at Maximum Weight Loss Temperature

NO.	RT/min	Name	CAS number	Relative peak area/%
1	1.96	Sulfur dioxide	7446-09-5	7.48
2	2.08	Furan	110-00-9	3.68
3	2.41	1,4-Pentadien-3-one	1890-28-4	4.33
4	3.05	Propanoic acid	79-09-4	0.56

5	3.32	Furan, 2,5-dimethyl-	625-86-5	0.40
6	3.53	2-Vinylfuran	1487-18-9	0.18
7	4.08	3,4-Pentadienal	4009-55-6	0.37
8	4.47	2(5H)-Furanone	497-23-4	0.54
9	4.67	Pentanal	110-62-3	0.31
10	5.13	Carbonocyanidic acid, ethyl ester	623-49-4	4.03
11	5.61	3-Furaldehyde	498-60-2	0.41
12	6.15	Furfural	98-01-1	6.30
13	6.39	2-Amino-1,3,5-triazine	4122-04-7	0.45
14	7.00	2-Furanmethanol	98-00-0	0.22
15	7.37	Furan, 2-propyl-	4229-91-8	1.18
16	8.04	4-Cyclopentene-1,3-dione	930-60-9	0.01
17	8.21	1-Propanone, 1-(2-furanyl)-	3194-15-8	0.57
18	9.17	Ethanone, 1-(2-furanyl)-	1192-62-7	1.67
19	9.76	6-Oxa-bicyclo[3.1.0]hexan-3-one	74017-10-0	0.95
20	10.59	2,5-Furandione, dihydro-3-methylene-	2170-03-8	0.50
21	11.10	Hydroquinone	123-31-9	0.18
22	11.58	2-Furancarboxaldehyde, 5-methyl-	620-02-0	1.04
23	12.01	Oxazole, 4,5-dihydro-2-methyl-	1120-64-5	0.06
24	12.14	2(5H)-Furanone, 3-methyl-	22122-36-7	0.22
25	12.23	1-Propanone, 1-(2-furanyl)-	3194-15-8	0.25
26	12.47	Phenol	108-95-2	0.31
27	12.53	Resorcinol	108-46-3	0.45
28	13.33	N-Butyl-tert-butylamine	16486-74-1	1.11
29	14.60	o-Cymene	527-84-4	0.64
30	15.17	1-Benzofuran-5-ol	13196-10-6	0.21
31	15.39	3-Cyclopropyl-3-oxopropanenitrile	118431-88-2	1.11
32	16.07	Phenol, 2-methyl-	95-48-7	0.32
33	16.81	1,2-Hexadiene, 5-methyl-	13865-36-6	0.30
34	17.19	p-Cresol	106-44-5	0.37
35	17.28	2-Octen-1-ol, (Z)-	26001-58-1	0.65
36	17.56	Phenol, 2-methoxy-	90-05-1	14.13
37	18.10	Tiglic acid	80-59-1	0.92
38	18.66	Levoglucosenone	37112-31-5	10.29
39	20.51	Benzene, 1,2-dimethoxy-	91-16-7	0.31
40	22.33	4-Methyl-2-oxopentanenitrile	66582-16-9	2.17
41	22.60	Creosol	93-51-6	1.79
42	22.92	2-Butene-1,4-diol, (Z)-	6117-80-2	0.43
43	23.60	1,4:3,6-Dianhydro-α-d-glucopyranose	~	5.11
44	24.23	3,4-Anhydro-d-galactosan	~	3.89
45	24.32	5-Hydroxymethylfurfural	67-47-0	1.59
46	24.91	3,4-Dimethoxytoluene	494-99-5	0.83
47	25.03	cis-1,2-Cyclohexanediol	1792-81-0	0.10
48	25.35	2,3-Anhydro-d-mannosan	~	0.78
49	25.59	2,3-Anhydro-d-galactosan	~	0.28
50	25.79	Methyl-α-d-ribofuranoside	~	1.81
51	26.52	Phenol, 4-ethyl-2-methoxy-	2785-89-9	0.72
52	28.15	2-Methoxy-4-vinylphenol	7786-61-0	1.28
53	28.68	Benzene, 4-ethyl-1,2-dimethoxy-	5888-51-7	0.07
54	29.78	Phenol, 2,6-dimethoxy-	91-10-1	0.29

55	30.61	Benzene, 4-ethenyl-1,2-dimethoxy-	6380-23-0	0.24
56	31.75	Vanillin	121-33-5	3.49
57	33.75	2,5-Cyclohexadiene-1,4-dione, 2,6-bis(1,1-dimethylethyl)-	719-22-2	2.16
58	34.08	Phenol, 2-methoxy-4-(1-propenyl)-	97-54-1	2.29
59	39.86	1,6-Anhydro-α-d-galactofuranose	~	3.67

Table S5. Volatile Pyrolysis Products of C2H1 at Maximum Weight Loss Temperature

NO.	RT/min	Name	CAS number	Relative peak area/%
1	1.99	Glyoxal	107-22-2	0.61
2	2.07	Furan	110-00-9	3.95
3	2.44	1,4-Pentadien-3-one	1890-28-4	5.55
4	2.78	Furan, 2,3-dihydro-	1191-99-7	0.54
5	2.85	1,3-Cyclohexadiene	592-57-4	1.06
6	3.03	4-Heptanol	589-55-9	0.78
7	3.18	3-Hexanone	589-38-8	0.56
8	3.30	Furan, 2,5-dimethyl-	625-86-5	0.81
9	3.55	2-Vinylfuran	1487-18-9	0.26
10	3.87	2,2'-Bifuran, 2,2',5,5'-tetrahydro-	98869-92-2	0.44
11	4.10	3,4-Pentadienal	4009-55-6	0.64
12	4.38	Cyclobutene, 2-propenylidene-	52097-85-5	1.05
13	4.68	Succindialdehyde	638-37-9	1.06
14	4.95	Cyclopentanone	120-92-3	0.42
15	5.14	Carbonocyanidic acid, ethyl ester	623-49-4	7.66
16	5.61	3-Furaldehyde	498-60-2	0.84
17	6.15	Furfural	98-01-1	14.63
18	6.39	2-Amino-1,3,5-triazine	4122-04-7	0.11
19	7.01	2-Furanmethanol	98-00-0	0.64
20	7.37	Furan, 2-propyl-	4229-91-8	1.86
21	8.04	4-Cyclopentene-1,3-dione	930-60-9	0.79
22	8.99	2-Cyclopenten-1-one, 2-methyl-	1120-73-6	0.48
23	9.17	Ethanone, 1-(2-furanyl)-	1192-62-7	2.66
24	9.75	6-Oxa-bicyclo[3.1.0]hexan-3-one	74017-10-0	3.36
25	10.49	2(5H)-Furanone, 5-methyl-	591-11-7	0.41
26	10.62	2,5-Furandione, dihydro-3-methylene-	2170-03-8	0.21
27	11.11	Hydroquinone	123-31-9	0.40
28	11.58	2-Furancarboxaldehyde, 5-methyl-	620-02-0	2.67
29	11.77	2-Butenal, 2-ethenyl-	20521-42-0	1.28
30	12.12	1-Propanone, 1-(2-furanyl)-	3194-15-8	0.80
31	12.53	Resorcinol	108-46-3	0.96
32	13.32	N-Butyl-tert-butylamine	16486-74-1	1.84
33	14.35	4H-1,2,4-Triazole, 3,4,5-trimethyl-	16759-45-8	0.17
34	14.60	Maleic hydrazide	123-33-1	1.99
35	15.20	1-Benzofuran-5-ol	13196-10-6	0.53
36	15.39	3-Cyclopropyl-3-oxopropanenitrile	118431-88-2	0.80

37	15.86	1,3-Dioxolan-2-one, 4,4,5,5-tetramethyl-	19424-29-4	0.88
38	16.81	1,2-Hexadiene, 5-methyl-	13865-36-6	0.52
39	17.05	3-Furancarboxylic acid, methyl ester	13129-23-2	0.02
40	17.13	Orcinol	504-15-4	0.73
41	17.27	2-Octen-1-ol, (Z)-	26001-58-1	0.81
42	17.35	Furyl hydroxymethyl ketone	17678-19-2	0.24
43	17.54	Furaneol	3658-77-3	1.87
44	18.11	Tiglic acid	80-59-1	1.35
45	18.69	Levoglucosenone	37112-31-5	11.12
46	22.35	4-Methyl-2-oxopentanenitrile	66582-16-9	2.95
47	22.93	2-Butene-1,4-diol, (Z)-	6117-80-2	0.97
48	23.64	1,4:3,6-Dianhydro-α-d-glucopyranose	~	5.43
49	24.32	5-Hydroxymethylfurfural	67-47-0	5.36
50	24.99	cis-1,2-Cyclohexanediol	1792-81-0	0.55
51	30.86	1-Naphthalenol, 1,2,3,4,4a,7,8,8a-octahydro-1,6-dimethyl-4-(1-methylethyl)-, [1R-(1α,4β,4aβ,8aβ)]-	19435-97-3	0.12
52	34.09	Pentanoic acid, 2,2,4-trimethyl-3-carboxyisopropyl, isobutyl ester	~	1.40
53	34.92	Benzophenone	119-61-9	0.43
54	37.81	β-D-Glucopyranose, 1,6-anhydro-	498-07-7	1.76
55	42.76	9H-Fluorene, 9-methylene-	4425-82-5	0.07
56	42.98	cyclohexane, 1,1'-[1,2-ethenediyl]bis-	~	0.66

Table S6. Volatile Pyrolysis Products of Hemicellulose at 350 °C

NO.	RT/min	Name	CAS number	Relative peak area/%
1	1.98	Glyoxal	107-22-2	1.76
2	2.10	Acetic acid, cyano-, 2-methoxyethyl ester	10258-54-5	7.20
3	2.35	(R)-(-)-Leucinol	53448-09-2	1.75
4	2.43	Furan, 2-methyl-	534-22-5	9.03
5	2.70	1,3-Cyclohexadiene	592-57-4	1.59
6	2.83	Urea, methyl-	598-50-5	0.78
7	2.99	Propanoic acid	79-09-4	0.48
8	3.17	3-Hexanone	589-38-8	0.73
9	3.28	Furan, 2,5-dimethyl-	625-86-5	1.26
10	3.87	2,2'-Bifuran, 2,2',5,5'-tetrahydro-	98869-92-2	1.43
11	3.97	Hex-4-yn-3-one	10575-41-4	1.40
12	4.37	Cyclobutene, 2-propenylidene-	52097-85-5	2.06
13	4.94	Cyclopentanone	120-92-3	3.97
14	5.64	Furfural	98-01-1	1.38
15	6.20	2-Cyclopenten-1-one	930-30-3	7.61
16	6.94	2-Furanmethanol	98-00-0	1.42
17	7.56	p-Xylene	106-42-3	0.95
18	8.40	2-Cyclopenten-1-one, 3-ethyl-	5682-69-9	0.83
19	8.98	2-Cyclopenten-1-one, 2-methyl-	1120-73-6	2.52
20	9.20	Ethanone, 1-(2-furanyl)-	497-23-4	2.53

21	10.21	2-Cyclohexen-1-one	930-68-7	0.93
22	10.42	2-Cyclopenten-1-one, 3,4-dimethyl-	30434-64-1	0.82
23	11.74	2-Cyclopenten-1-one, 3-methyl-	2758-18-1	2.47
24	12.26	2(5H)-Furanone, 3-methyl-	22122-36-7	0.92
25	12.49	Phenol	108-95-2	1.89
26	14.58	1,2-Cyclopentanedione, 3-methyl-	765-70-8	2.26
27	15.13	2-Cyclopenten-1-one, 2,3-dimethyl-	1121-05-7	2.59
28	15.68	Pyrrolidine, 1-methyl-	120-94-5	2.23
29	16.05	Phenol, 2-methyl-	95-48-7	2.69
30	17.17	Phenol, 3-methyl-	108-39-4	2.97
31	17.82	Cyclohexanone, 4-hydroxy-	13482-22-9	18.29
32	18.65	Benzene, 1-methoxy-4-methyl-	104-93-8	0.56
33	19.63	2(3H)-Furanone, 5-butyldihydro-	104-50-7	1.38
34	22.92	Catechol	120-80-9	0.82
35	23.65	1,4:3,6-Dianhydro-α-d-glucopyranose	~	2.65
36	26.66	1H-Inden-1-one, 2,3-dihydro-	83-33-0	1.54
37	40.83	Phenol, 3,5-bis(1,1-dimethylethyl)-	1138-52-9	4.32

Table S7. Volatile Pyrolysis Products of Lignin at 260 °C

NO.	RT/min	Name	CAS number	Relative peak area/%
1	1.95	Sulfur dioxide	7446-09-5	35.98
2	2.46	Furan, 2-methyl-	534-22-5	2.13
3	17.59	Phenol, 2-methoxy-	90-05-1	21.38
4	31.79	Vanillin	121-33-5	37.00
5	35.41	Apocynin	498-02-2	3.51

Table S8. Volatile Pyrolysis Products of L2H1 at Maximum Weight Loss Temperature

NO.	RT/min	Name	CAS number	Relative peak area/%
1	1.98	Sulfur dioxide	7446-09-5	20.96
2	2.13	Dimethyl sulfide	75-18-3	3.58
3	2.43	Furan, 2-methyl-	534-22-5	2.15
4	3.89	Disulfide, dimethyl	624-92-0	0.76
5	4.35	Toluene	108-88-3	0.33
6	4.96	Cyclopentanone	120-92-3	0.23
7	5.62	Furfural	98-01-1	0.36
8	6.23	2-Cyclopenten-1-one	930-30-3	2.35
9	9.02	2-Cyclopenten-1-one, 2-methyl-	1120-73-6	0.38
10	9.22	Ethanone, 1-(2-furanyl)-	1192-62-7	0.58
11	11.82	Dimethyl trisulfide	3658-80-8	0.53
12	12.47	Phenol	108-95-2	1.35
13	14.61	p-Cymene	99-87-6	0.69
14	15.19	2-Cyclopenten-1-one, 2,3-dimethyl-	1121-05-7	0.32
15	16.05	Phenol, 3-methyl-	108-39-4	0.61
16	17.15	p-Cresol	106-44-5	0.62

17	17.57	Phenol, 2-methoxy-	90-05-1	31.84
18	17.87	Cyclohexanone, 4-hydroxy-	13482-22-9	5.82
19	20.52	Benzene, 1,2-dimethoxy-	91-16-7	0.86
20	21.96	2-Methoxy-6-methylphenol	2896-67-5	0.34
21	22.37	1,3-Benzenediol, 4-ethyl-	2896-60-8	0.24
22	22.6	Creosol	93-51-6	3.75
23	23.67	1,4:3,6-Dianhydro-α-d-glucopyranose	~	0.57
24	24.89	3,4-Dimethoxytoluene	494-99-5	0.78
25	26.53	Phenol, 4-ethyl-2-methoxy-	2785-89-9	1.50
26	28.15	2-Methoxy-4-vinylphenol	7786-61-0	2.45
27	28.66	Benzene, 4-ethyl-1,2-dimethoxy-	5888-51-7	0.28
28	29.76	Phenol, 2,6-dimethoxy-	91-10-1	0.67
29	30.6	Benzene, 4-ethenyl-1,2-dimethoxy-	6380-23-0	0.30
30	31.76	Vanillin	121-33-5	6.11
31	34.00	Phenol, 2-methoxy-4-(1-propenyl)-	97-54-1	0.74
32	35.35	Apocynin	498-02-2	4.25
33	40.43	Benzophenone	119-61-9	3.04
34	40.82	Phenol, 3,5-bis(1,1-dimethylethyl)-	1138-52-9	0.66

Table S9. Volatile Pyrolysis Products of C2L2H1 at Maximum Weight Loss Temperature

NO.	RT/min	Name	CAS number	Relative peak area/%
1	1.96	Sulfur dioxide	7446-09-5	11.43
2	2.08	Furan	110-00-9	3.60
3	2.34	(R)-(-)-Leucinol	53448-09-2	1.97
4	2.45	1,4-Pentadien-3-on	1890-28-4	3.70
5	2.86	1,3-Cyclohexadiene	592-57-4	0.18
6	3.03	Propanoic acid	79-09-4	0.23
7	3.31	Furan, 2,5-dimethyl-	625-86-5	0.47
8	3.52	2-Vinylfuran	1487-18-9	0.21
9	3.87	2,2'-Bifuran, 2,2',5,5'-tetrahydro-	98869-92-2	0.52
10	4.11	3,4-Pentadienal	4009-55-6	0.36
11	4.45	2(5H)-Furanone	497-23-4	0.71
12	4.67	Pentanal	110-62-3	0.51
13	5.13	Carbonocyanidic acid, ethyl ester	623-49-4	3.54
14	5.63	3-Furaldehyde	498-60-2	0.47
15	6.15	Furfural	98-01-1	6.83
16	6.40	2-Amino-1,3,5-triazine	4122-04-7	0.02
17	6.99	2-Furanmethanol	98-00-0	0.39
18	7.37	Furan, 2-propyl-	4229-91-8	1.87
19	8.04	4-Cyclopentene-1,3-dione	930-60-9	0.46
20	8.21	1-Propanone, 1-(2-furanyl)-	3194-15-8	0.14
21	8.38	2-Cyclopenten-1-one, 3-ethyl-	5682-69-9	0.17
22	9.01	2-Cyclopenten-1-one, 2-methyl-	1120-73-6	0.34
23	9.17	2(5H)-Furanone	497-23-4	1.82
24	9.76	6-Oxa-bicyclo[3.1.0]hexan-3-one	74017-10-0	0.88
25	10.50	2(5H)-Furanone, 5-methyl-	591-11-7	0.19
26	10.61	2,5-Furandione, dihydro-3-methylene-	2170-03-8	0.18

27	11.11	Hydroquinone	123-31-9	0.39
28	11.57	2-Furancarboxaldehyde, 5-methyl-	620-02-0	1.68
29	11.79	2-Butenal, 2-ethenyl-	20521-42-0	0.74
30	12.15	2(5H)-Furanone, 3-methyl-	22122-36-7	0.72
31	12.48	Phenol	108-95-2	0.53
32	12.53	Resorcinol	108-46-3	0.60
33	13.34	N-Butyl-tert-butylamine	16486-74-1	1.06
34	14.63	o-Cymene	527-84-4	0.78
35	15.15	1-Benzofuran-5-ol	13196-10-6	0.26
36	15.38	3-Cyclopropyl-3-oxopropanenitrile	118431-88-2	0.88
37	16.06	Phenol, 2-methyl-	95-48-7	0.29
38	16.81	1,2-Hexadiene, 5-methyl-	13865-36-6	0.30
39	17.22	p-Cresol	106-44-5	0.42
40	17.27	2-Octen-1-ol, (Z)-	26001-58-1	0.45
41	17.56	Phenol, 2-methoxy-	90-05-1	14.69
42	17.87	Cyclohexanone, 4-hydroxy-	13482-22-9	3.50
43	18.10	Tiglic acid	80-59-1	0.50
44	18.69	Levoglucosenone	37112-31-5	5.55
45	20.52	Benzene, 1,2-dimethoxy-	91-16-7	0.42
46	21.96	2-Methoxy-6-methylphenol	2896-67-5	0.14
47	22.34	4-Methyl-2-oxopentanenitrile	66582-16-9	1.34
48	22.61	Creosol	93-51-6	1.71
49	22.93	2-Butene-1,4-diol, (Z)-	6117-80-2	0.44
50	23.61	1,4:3,6-Dianhydro-α-d-glucopyranose	~	2.79
51	24.26	3,4-Anhydro-d-galactosan	~	2.16
52	24.89	3,4-Dimethoxytoluene	494-99-5	0.52
53	25.38	2,3-Anhydro-d-mannosan	~	0.30
54	25.60	2,3-Anhydro-d-galactosan	~	0.10
55	26.53	Phenol, 4-ethyl-2-methoxy-	2785-89-9	0.87
56	28.16	2-Methoxy-4-vinylphenol	7786-61-0	1.69
57	28.68	Benzene, 4-ethyl-1,2-dimethoxy-	5888-51-7	0.44
58	29.78	Phenol, 2,6-dimethoxy-	91-10-1	0.32
59	30.61	Benzene, 4-ethenyl-1,2-dimethoxy-	6380-23-0	0.39
60	31.76	Vanillin	121-33-5	3.58
61	33.67	2,5-Cyclohexadiene-1,4-dione, 2,6-bis(1,1-dimethylethyl)-	719-22-2	1.58
62	34.02	Phenol, 2-methoxy-4-(1-propenyl)-	97-54-1	1.26
63	39.93	1,6-Anhydro-α-d-galactofuranose	~	4.79
64	40.65	Benzophenone	119-61-9	0.59